Maintenance of hemiround colonies and undifferentiated state of mouse induced pluripotent stem cells on carbon nanotube-coated dishes

Tsukasa Akasaka[a,*], Atsuro Yokoyama[a], Makoto Matsuoka[a], Takeshi Hashimoto[b] and Fumio Watari[a]

[a]*Graduate School of Dental Medicine, Hokkaido University, Kita 13, Nishi 7, Kita-ku, Sapporo 060-8586, Japan*

[b]*Meijo Nano Carbon Co. Ltd., Otsubashi bldg. 4F, 3-4-10 Marunouchi, Naka-ku, Nagoya 460-0002, Japan*

[*]Corresponding author

Tel/Fax: +81 11 706 4251

E-mail address: akasaka@den.hokudai.ac.jp (T. Akasaka)

Abstract

Induced pluripotent stem (iPS) cells have attracted worldwide interest. However, there have been only a few studies investigating effective culture substrates for feeder-free culturing for the maintenance of iPS cells. In this study, we cultured mouse iPS cells under feeder-free conditions on carbon nanotube (CNT)-coated dishes and then evaluated the colony morphology and differentiation state of the cells on the dishes. After 5 d of cultivation in a medium containing 15% fetal bovine serum (FBS) and leukemia inhibitory factor (LIF), the colonies on thick films of multi-walled CNTs (MWCNTs) were observed to be hemiround; further, the cells expressed early undifferentiation markers. On the other hand, the colonies on a cell culture polystyrene dish and a collagen-coated polystyrene dish showed indistinct outline and spread well, and most spreading cells only weakly expressed early undifferentiation markers. These results indicate that the thick films of MWCNTs could maintain hemiround colonies and undifferentiated state of mouse iPS cells cultured under feeder-free conditions.

1. Introduction

Mouse induced pluripotent stem (iPS) cells have been established from mouse fibroblasts through reprogramming by introducing a combination of 4 defined transcription factors, Oct3/4, Sox2, Klf4, and c-Myc [1,2]. iPS cells have attracted worldwide interest; they will be one of the most promising sources for research in the life sciences and for regeneration therapy [3–5]. In addition, iPS cells will be used for applications to assay systems evaluating the efficacy and toxicity of drugs [4]. To date, iPS cells have usually been cultured on feeder cells such as mouse embryonic fibroblast (MEF) cells or those of a mouse fibroblast STO cell line transformed with neomycin resistance and murine leukemia inhibitory factor (LIF) genes (SNL cells) [1,3,6]. Recently, several separated-feeder-cell or feeder-free conditions for culturing iPS cells have been reported to avoid several problems arising because of the coexistence of feeder cells. Abraham et al. reported the propagation of iPS cells in a microporous membrane-based indirect co-culture system [7]. In this system, iPS cells can be propagated and their pluripotency can be maintained while preventing their mixing with feeder cells. This system will enable testing of novel feeder cells and conduction of differentiation studies using co-culture with other cell types and will simplify stepwise

changes in culture conditions for staged-differentiation protocols. Alternatively, Matrigel-coated substrates [8–10] and gelatin-coated substrates [11,12] have been used for with feeder-free culturing of iPS cells, in the presence of LIF for mouse iPS cells or fibroblast growth factor (FGF) for human iPS cells. Gelatin-coated substrates have also been used in feeder-free culturing of mouse iPS cells to eliminate contamination by feeder cells [12]. Kitajima and Niwa have reported a feeder-free culture system of human iPS cells [11]. This system is based on the combinatorial use of Rho-associated kinase (ROCK) inhibitor and soluble fibronectin on a gelatin-coated surface under feeder-free conditions and is suitable for large-scale and cost-effective culture of human iPS cells. In a previous study, an embryoid body (EB) of human iPS cells in low-cell-binding dishes was harvested in serum-free media on a feeder-free poly-D-lysine-/laminin-/fibronectin-coated substrate for not only the maintenance but also the differentiation assay of iPS cells [13]. In this case, the coating could support the adhesion of iPS cells to the substrate in the serum-free media. Thus, development of substrates for feeder-free culturing can improve iPS cell culture since feeder cells cause variability and limitations in experimental results. Moreover, a variety of functional substrates can allow easy assays of toxicity and control of differentiation of iPS cells; these substrates are valuable for future application to pharmaceutical screening and cell

replacement therapy.

Carbon nanotubes (CNTs) are a candidate for multifunctional biomaterials for a variety of biological applications [14–21]. CNTs are structural carbon fiber composites found in 2 structural forms: single-walled CNTs (SWCNTs) and multi-walled CNTs (MWCNTs). SWCNTs can be considered as long wrapped graphene sheets with diameters typically ranging from 0.5 to 1.5 nm. MWNCTs have larger diameters typically ranging from 10 to 100 nm owing to their multilayered structures. Mattson et al. reported the first application of CNTs as a scaffold for the growth of nerve cells [15]. They suggested that CNTs act as a cell culture substrate at the nanometer scale, which is similar to the size of small nerve fibers, filopodia, and synaptic contact. In a recent study, we showed that surface roughness of CNT films used as a cell culture scaffold largely influenced the morphology of osteoblast-like cells (Saos-2) [22]. In particular, the cells on the rough surface of thick MWCNT films tended to spread lesser than those on the smooth surface of thin MWCNT films. Similar morphological changes have been reported in osteoblast-like cells (Saos-2) on MWCNT constructs [23]; human cervical carcinoma cells (HeLa) on MWCNT scaffolds [24]; and human lung epithelial cells (A549), osteoblast-like cells (MG63), and primary/fetal osteoblasts (FOBs) on MWCNT surfaces [25]. These studies indicate that surface roughness of CNTs could

possibly control the morphology of certain kinds of cells, depending on the culture conditions. In addition, one of the advantages of MWCNT films is that a nano-surface structure can easily be prepared on the surface of various substrates by simple coating, which provides a grip for cells because of its 3D network [26,27]. Furthermore, CNT films show a mild response to cells owing to their graphite structure [28,29], compared with the general biomaterials with functional groups such as -OH, -COOH, and -NH_2. Carbon materials are generally considered prospective biomedical materials owing to their excellent compatibility with the blood, soft tissue, and bones [30–32]. Further, they show the properties of both bioinertness and chemical stability, essential for artificial heart valve and dental implants in the body [33,34]. Therefore, CNTs composed of graphene sheets can be one of the candidates as cell culture substrates for iPS cells because of their nano-roughness which facilitates adhesion, bioinertness, chemical stability, and compatibility.

However, only a few results regarding the culture of only limited types of cells on CNT scaffolds have been reported. In addition, investigations related to morphological changes in and maintenance of embryonic stem (ES) cells, particularly iPS cells, on CNT scaffolds have not been conducted. Several researchers have reported the toxicity of CNTs for ES cells [35] and their differentiation on CNT sheets [36,37].

One possibility is that iPS cells might adhere to rough surface of CNT films and hence spread less and the cells might respond mildly compared with popular matrices for iPS cells culturing because of the graphite structure of CNT films. In this study, we investigated cell adhesion, colony morphology, and differentiation of mouse iPS cells cultured on CNT-coated dishes, using a cell culture polystyrene dish and a collagen-coated polystyrene dish as the control popular matrix for general cell culture and for the culturing of iPS and ES cells. In addition, cell growth of MEF-1 cells on CNT-coated dishes was also investigated.

2. Materials and methods

2.1 *Preparation of CNT-coated dishes*

CNTs employed in this study and preparation of CNT-coated dishes were as previously described [22]. Purification and preparation methods in brief are as follows. Purified SWCNTs (diameter, 0.8–2.5 nm) were purchased from Meijo Nano Carbon Co. Ltd. (Nagoya, Japan); they were synthesized using the arc discharge method [38]. MWCNTs were purchased from NanoLab Inc. (Brighton, MA, USA); they were synthesized using the chemical vapor deposition technique. The MWCNTs (average diameter, 30 nm) were purified by a previously described method [39]. The SWCNTs had a purity of >95 wt.% and contained <5 wt.% amorphous carbon as the dominant impurity; on the other hand, the MWCNTs had a purity of >98 wt.% and contained <2 wt.% amorphous carbon. To prepare the homogeneous CNT coating, a dilute solution of CNTs in dehydrated ethanol was dispersed by ultrasonication. An aliquot of the dispersed CNT solution was immediately spotted onto a non-treated polystyrene dish (Normal PS; diameter, 60 mm) and dried. This procedure was repeated until the necessary amount of CNT coating was obtained. All dishes thus prepared were dried and sterilized by

ultraviolet (UV) irradiation for 1 d.

The following abbreviations have been used for the CNT-coated dishes used in this study: SWCNT-coated dishes, SWCNT0.5 (0.5 μg/cm^2); MWCNT-coated dishes, MWCNT0.5 (0.5 μg/cm^2) and MWCNT5 (5 μg/cm^2). For comparison, we used the following commercially available polystyrene dishes (diameter, 60 mm): Normal PS (Corning Inc., NY, USA), cell culture polystyrene dish (Culture PS; Corning Inc.), and collagen-coated polystyrene dish (Collagen PS; 25020 COL1; Iwaki Co. Ltd., Tokyo, Japan).

2.2 *Surface characteristics*

For observation under a scanning electron microscope (SEM; S-4000; Hitachi High-Tech Fielding Corp., Tokyo, Japan), the dishes were coated with Pt-Pd by a sputtering apparatus (E-1030; Hitachi High-Tech Fielding Corp., Tokyo, Japan). And then, SEM images of the surface of the dishes were obtained.

To evaluate surface roughness, the CNT-coated dishes were characterized by using atomic force microscopy (AFM). AFM was performed using a commercial Nanoscope IIIa (Veeco Instruments Inc, Santa Barbara, CA, USA) in the tapping mode

across an area (2 μm × 2 μm) of the sample surface using a silicon cantilever (Tap300 Metrology probe; MRP-11100, Veeco Instruments Inc., Woodbury, NY, USA). Gwyddion data analysis software covered by the GNU general public license was used for AFM image analysis. The roughness of the surface was assessed by measuring the roughness parameter, R_a (roughness average). Values were expressed as the mean and standard error of 3 experiments.

To estimate the surface wettability of the dishes, we measured contact angles of water drop on the surface of the dishes. The CNT-coated dishes sterilized by UV irradiation were used for measurement of contact angles. Ultrapure water (Kanto Chemical Co., Inc., Tokyo, Japan) drops (2 μL) were placed on the surface of the dishes in an ambient environment. Contact angles were measured on a digital microscope (VH-6300; Keyence, Osaka, Japan). Images of water spreading were recorded with CCD camera after 10 s and saved onto a PC, and automated contact angle measurements were performed using ImageJ plug-in LB-ADSA [40]. Values were expressed as the mean and standard error of 10 experiments.

2.3 *Cell culture*

MEF-derived mouse iPS cell line iPS-MEF-Ng-20D-17 [1,2] was purchased from RIKEN BioResource Center (RIKEN BRC; Tsukuba, Japan). The cells were seeded in StemMedium (DS Pharma Biomedical Co. Ltd., Osaka, Japan) supplemented with 1,000 U/mL of mouse LIF (ESGRO; Millipore Co., Bedford, MA, USA) and incubated at 37°C in a humidified 5% CO_2/95% air atmosphere for 6 d. After complete removal of the medium and washing 3 times with phosphate-buffered saline (PBS), the cells were dissociated with 0.25% trypsin/1 mM ethylenediaminetetraacetic acid (EDTA) and incubated at 37°C for 10 min. Thereafter, they were centrifuged at 1,000 *g* and the supernatant was removed. The cells were frozen using a freezing solution for ES cells (ReproCELL Inc., Tokyo, Japan) according to the instructions given in the manual provided by the manufacturer. In the subsequent experiences, the mouse iPS cells were used at 2 passages from purchase.

2.4 *Cell adhesion test*

To estimate the ability of cell adhesion on the CNT-coated dishes, we carried out a cell adhesion test [41]. The dishes were precoated with 4 mL of Dulbecco's modified Eagle's medium (DMEM; D5796; Sigma-Aldrich Co. Ltd., St. Louis, MO, USA)

containing 15% FBS (CELLect, Lot no. 5564J; MP Biomedicals Inc., Aurora, OH, USA), 0.1 mM nonessential amino acids (NEAA), and 0.1 mM 2-mercaptoethanol and supplemented with 1,000 U/mL of LIF, at 37°C in a humidified 5% CO_2/95% air atmosphere for 1h prior to cell seeding. Mouse iPS cells were then seeded at a density of 30,000 cells/cm^2 (0.47 μg/mL as a DNA).

After 1 h of incubation, the dishes were washed 3 times with PBS. The cells adhered on the dishes were lysed in 4 mL of Tris buffer (pH 7; 10 mM Tris base, 1 mM EDTA, and 0.1% Triton X-100) by shaking for 30 min at 4°C. Cell adhesion was estimated by the PicoGreen DNA assay (Molecular Probes, Leiden, Netherlands), by measuring the fluorometric double-stranded DNA (dsDNA) content [42] according to the manufacturer's instructions. The fluorescence of the lysate was measured using a fluorescence spectrophotometer (F-2500; Hitachi, Tokyo, Japan) at an excitation wavelength of 480 nm and an emission wavelength of 520 nm. Values were expressed as the mean and standard error of the DNA content of adherent cells of each dish. For a SEM observation, the dishes cultured for 12 h were rinsed with PBS to remove the non-adherent cells, fixed in a solution of 2.5% glutaraldehyde, and post-fixed in 1% osmium tetroxide. Thereafter, they were dehydrated in a graded series of alcohol (50%, 70%, 80%, 90%, 95%, and 100%) and then subjected to critical point drying at 37°C.

After Pt-Pd coating, SEM images were obtained.

2.5 *Cell culture assay and examination of colony morphology*

To estimate the ability of cell growth on the CNT-coated dishes, we carried out a cell culture assay [22]. The dishes were precoated with 4 mL of DMEM containing 15% FBS, 0.1 mM NEAA, and 0.1 mM 2-mercaptoethanol and supplemented with 1,000 U/mL of LIF, at 37°C in a humidified 5% CO_2/95% air atmosphere for 1 h. Mouse iPS cells were then seeded at a density of 30,000 cells/cm^2 (0.47 μg/mL as a DNA) and cultured in the abovementioned medium. The medium was replaced every day. After 5 d, the medium was removed and the dishes were washed with PBS. The DNA content of cells cultured on the dishes was estimated by the PicoGreen DNA assay as mentioned above. For optical microscope observations, the Nikon ECLIPSE TS100 microscope (Nikon Co., Ltd., Tokyo, Japan) was used, and digital images were acquired using a Nikon DS-5M-L1 camera (Nikon Co. Ltd.). SEM observations were carried out by a similar procedure as mentioned above.

2.6 *Alkaline phosphatase (ALP) staining and immunocytochemical analysis*

ALP staining was performed using an ALP detection kit (Chemicon International Inc., Temecula, CA, USA) according to the manufacturer's instructions. In brief, mouse iPS cells cultured for 5 d were fixed in 4% neutral-buffered formalin solution (Wako Pure Chemical Industries Ltd., Osaka, Japan) at room temperature for 1 min, washed with rinse buffer (20 mM Tris-HCl, pH 7.4, 0.15 M NaCl, and 0.05% Tween-20), and then incubated with ALP staining solution (naphthol/fast red violet) at room temperature for 30 min. Cells positive for ALP activity were stained red. Color development was examined using the Nikon ECLIPSE TS100 microscope, and digital images were acquired using the Nikon DS-5M-L1 camera under the same conditions, which were manually set, for all samples.

For fluorescence microscope observations, mouse iPS cells cultured for 5 d were fixed in 4% paraformaldehyde in PBS for 30 min at 4°C. Thereafter, the cells were washed 3 times with PBS and permeabilized in PBS containing 0.2% Triton X-100 for 15 min at room temperature. The cells were rewashed 3 times with PBS containing 2% FBS, following which they were incubated overnight with anti-mouse OCT3/4 Alexa Fluor 488 (dilution, 1:50; eBioscience Inc., San Diego, CA, USA) and anti-mouse Nanog Alexa Fluor 647 (dilution, 1:500; eBioscience Inc.) in PBS containing 2% FBS

at 4°C. After staining, the cells were washed 3 times with PBS containing 2% FBS. For nuclear staining, 1 μg/mL of 4′,6-diamidino-2-phenylindole (DAPI) in PBS was added and the cells were incubated for 10 min at room temperature. Images were acquired using a fluorescence microscope (Biorevo BZ-9000; Keyence Corp., Osaka, Japan).

2.7 *MEF-1 cell culture assay*

MEF-1 (European Collection of Animal Cell Cultures [ECACC] no. 98061101; DS Pharma Biomedical Co. Ltd.) cells were seeded onto the CNT-coated dishes at a density of 1,000 cells/cm^2 (0.015 μg/mL as a DNA). The cells were cultured in 4 mL of DMEM with 10% FBS, 2 mM glutamine, and 1% penicillin-streptomycin-neomycin (PSN) antibiotic mixture (Invitrogen, Carlsbad, CA, USA) at 37°C in a humidified 5% CO_2/95% air environment. The medium was replaced every 2 d. After 5 d, the medium was removed and the dishes were washed with PBS. The DNA content of cells cultured on the dishes was estimated by the PicoGreen DNA assay as mentioned above.

2.8 *Statistical analysis*

Student's *t* test was used to determine intergroup differences and assess the statistical significance of the results. Statistical analysis was performed using the Microsoft Excel software, at a confidence level of 95%.

3. Results

3.1 *Surfaces of CNT-coated dishes*

In the present study, we prepared CNT-coated dishes by coating the surface of commercially available Normal PS with homogeneous thin or thick films of unmodified CNTs, as previously described [22]. Fig. 1 shows the SEM images of the surfaces of the CNT-coated (Fig. 1b, c, and d) and commercially available dishes used as the control (Fig. 1a, e, and f). The surface topography of the CNT-coated dishes was observed to be the same as previously reported [22]. In brief, a large area of the surface of the base substrate in SWCNT0.5 and MWCNT0.5 was exposed. The SWCNT0.5 films formed a fine network, while the MWCNT0.5 films formed a partially dense network on the surfaces of the dishes, as shown in Fig. 1b and c, respectively. In MWCNT5, the CNTs formed a densely packed 3D meshwork nanostructure that covered the entire surface (Fig. 1d). In Normal PS, Culture PS, and Collagen PS, the surfaces showed a flat topography (Fig. 1a, e, and f, respectively).

Table 1 shows the surface roughness (R_a) and contact angle of water drop on the surface of the dishes. The surface roughness of the SWCNT0.5 and MWCNT0.5

dishes was 6.9 ± 0.7 nm and 7.9 ± 1.8 nm, respectively. The surface roughness of the MWCNT5 dishes was 49.0 ± 2.5 nm. The R_a values of the thin SWCNT0.5 and MWCNT0.5 films tended to be similar. The surface of the thick MWCNT5 films was rougher than those of SWCNT0.5 and MWCNT0.5. The surface roughness of Normal PS, Culture PS, and Collagen PS was 1.9 ± 0.2 nm, 2.0 ± 0.3 nm, and 2.7 ± 0.4 nm, respectively. The R_a values of their surfaces indicate flatter than those of CNT-coated dishes. Contact angle of SWCNT0.5, MWCNT0.5, and MWCNT5 was 88.3 ± 1.1°, 87.2 ± 2.1°, and 113.1 ± 1.5°, respectively. Because a higher contact angle indicates higher hydrophobicity, all CNT-coated dishes exhibited hydrophobicity. In particular, MWCNT5 indicated the highest hydrophobicity among all the dishes. Contact angle of Normal PS, Culture PS, Collagen PS was 76.8 ± 0.7°, 61.7 ± 1.3°, and 44.8 ± 1.7°, respectively. Although the surface of Normal PS exhibited hydrophobicity, the surface of Culture PS and Collagen PS exhibited hydrophilicity.

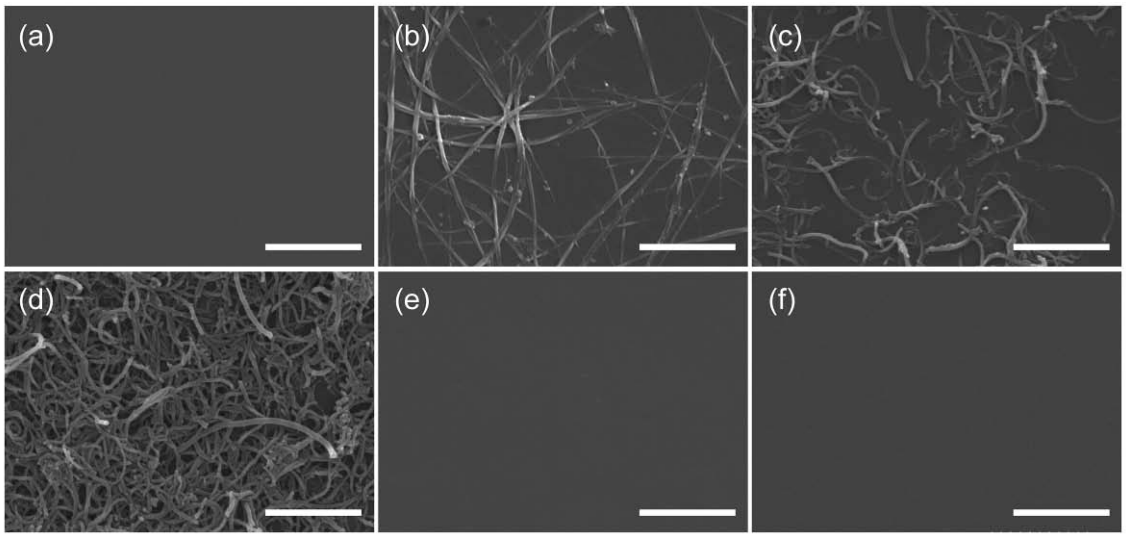

Fig. 1

Table 1. Surface roughness and contact angle of the dish substrates.

	Normal PS	SWCNT0.5	MWCNT0.5	MWCNT5	Culture PS	Collagen PS
R_a (nm)	1.9 ± 0.2	6.9 ± 0.7	7.9 ± 1.8	49.0 ± 2.5	2.0 ± 0.3	2.7 ± 0.4
Contact angle (°)	76.8 ± 0.7	88.3 ± 1.1	87.2 ± 2.1	113.1 ± 1.5	61.7 ± 1.3	44.8 ± 1.7

3.2 *Cell adhesion assay and morphology at an early stage*

To estimate the cell adhesion ability, mouse iPS cells were incubated on the dishes for 1 h in the presence of 15% FBS and LIF. Fig. 2 shows the DNA content of adherent cells

on various types of dishes, estimated using the PicoGreen DNA assay. Statistical analysis revealed that the DNA content of adherent cells on MWCNT5 was about 3.6–8.7 times greater than that on Normal PS, SWCNT0.5, and MWCNT0.5 ($p < 0.05$). The DNA content of adherent cells on SWCNT0.5 and MWCNT0.5 showed low similarity to that on Normal PS. Although the DNA content of adherent cells on MWCNT5 showed high similarity to that on Culture PS (no significant difference, $p > 0.05$), it was lower than that on Collagen PS ($p < 0.05$). The highest DNA content of adherent cells was found on Collagen PS. Fig. 3 shows the SEM images exhibiting the morphology of mouse iPS cells adhering to MWCNT5, Culture PS and Collagen PS after 12 h of incubation. Interestingly, most of cells on the Culture PS and the Collagen PS were flat and well spread in all directions, except the round cells overriding the flat cells (Fig. 3b and c); however, the cells on MWCNT5 did not appear to be well spread and exhibited round cytoplasmic extensions (Fig. 3a).

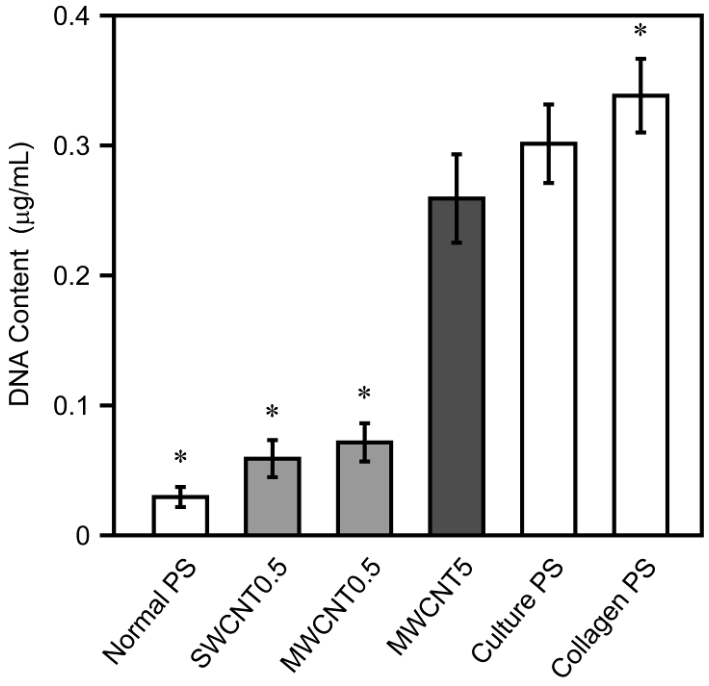
0.4
0.3
0.2
0.1
0
DNA Content (μg/mL)
*
*
*
*
Normal PS
SWCNT0.5
MWCNT0.5
MWCNT5
Culture PS
Collagen PS

Fig. 2

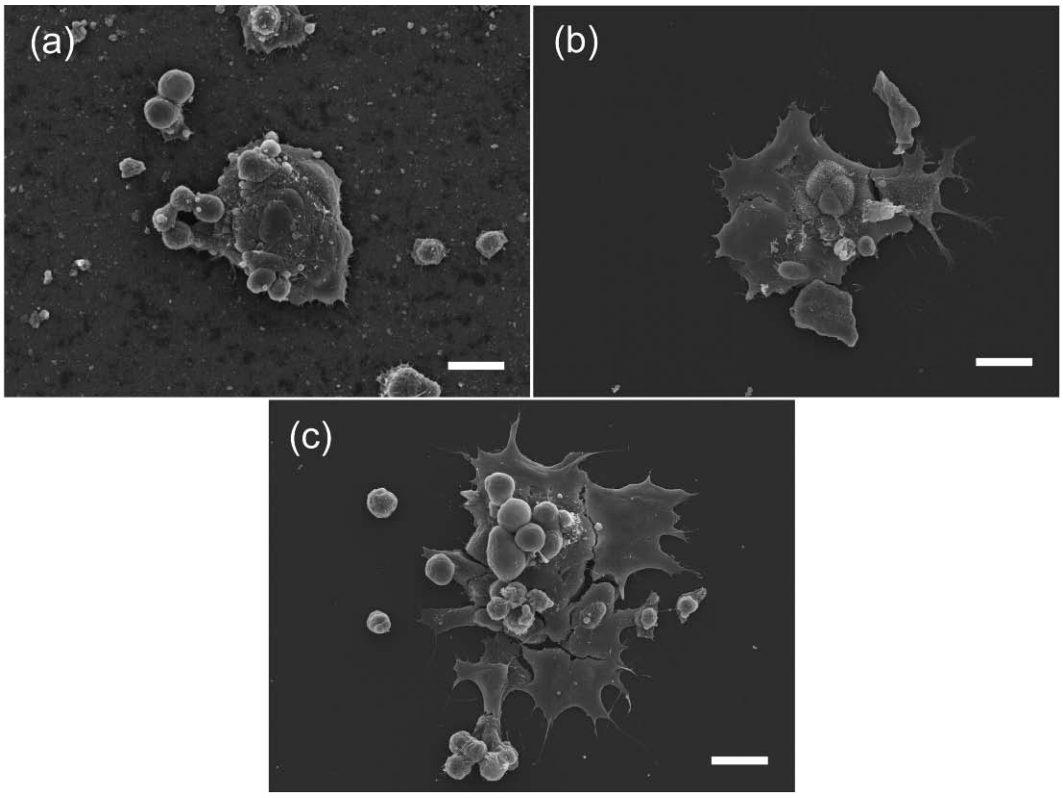
(a)
(b)
(c)

Fig. 3

3.3 *Cell morphology and growth*

To examine the colony morphology and evaluate the cell growth of mouse iPS cells cultured on various types of dish substrates, the cells were cultured directly on the CNT-coated dishes in a medium containing 15% FBS and LIF under feeder-free conditions.

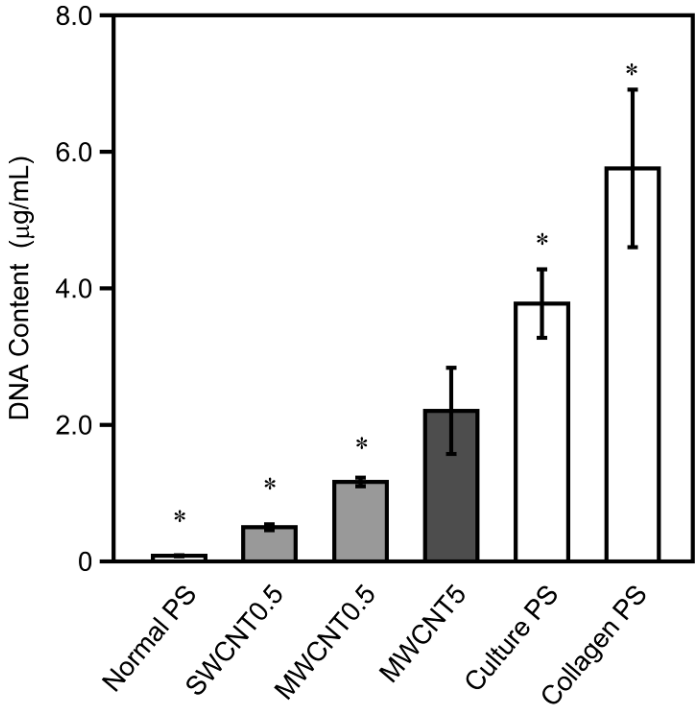

Fig. 4

Fig. 4 shows the DNA content of mouse iPS cells cultured on the surfaces of various types of dishes for 5 d. Cell growth was assayed by DNA content on the dishes. While the DNA content of cells cultured on both Collagen PS and Culture PS was greater than that on the CNT-coated dishes, the DNA content of cells cultured on the CNT-coated dishes was greater than that on Normal PS. Although the DNA content of cells cultured on MWCNT5 was the greatest among the CNT-coated dishes ($p < 0.05$), the DNA content of cells cultured on Collagen PS was the greatest among all the dishes. DNA content of cells cultured on Collagen PS was 2.6 times greater than that on MWCNT5 ($p < 0.05$). Compared with DNA content of cells cultured on Normal PS, DNA content of cells cultured of the mouse iPS cells on the CNT-coated dishes was more since the dishes were prepared from Normal PS by CNT coating.

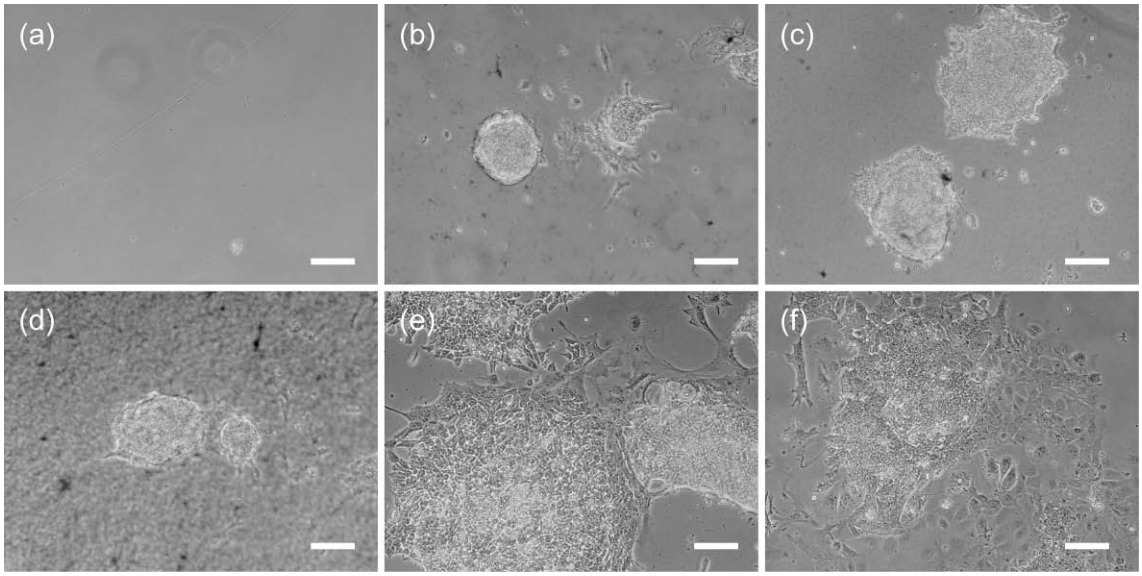

Fig. 5

Fig. 5 shows the representative colony morphologies of mouse iPS cells cultured on various types of dishes, as observed under an optical microscope. Colonies of iPS cells were observed on all the dishes, except Normal PS; this was because the cells were lost during medium change because of their weak adhesion due to the non-adhesive property of Normal PS. Interestingly, the mouse iPS cells formed hemiround and multicellular clusters approximately 100–200 μm in diameter on the CNT-coated dishes after 5 d of incubation. These colonies had clear edges and morphology similar to the typical ES cell-like morphology [43]. Both Fig. 4 and 5 show that the hemiround colonies were mostly formed on MWCNT5 among the CNT-coated dishes. Similar morphology of hemiround colonies was also observed on SWCNT0.5

and MWCNT0.5, however there were considerably few numbers of colonies formed on SWCNT0.5 and MWCNT0.5. On the other hand, the iPS colonies on both Culture PS and Collagen PS were partially raised spreading of many peripheral cells (Fig. 5e and f); however, DNA content of cells cultured on both the above dishes was high (Fig. 4). Fig. 6b, d, and e shows the SEM images of the representative colonies on MWCNT5, Culture PS, and Collagen PS at high magnification. A few filopodia of the cells extended to the MWCNT network on the dish (Fig. 6b), while numerous filopodia of the spread cells extended on the surface of Culture PS and Collagen PS (Fig. 6d and f). The SEM image at high magnification reveals that the colonies growing on MWCNT5 were hemiround, uniformly concentric, compact, and raised, which is the characteristic morphology of undifferentiated mouse iPS cells. Further, the colonies on MWCNT5 seemed to be slightly anchored to the MWCNT network. On the other hand, the SEM image of the cells on Culture PS and Collagen PS, acquired at high magnification, shows the presence of many filopodia extending from the cell body to the substrate (Fig. 6d and f). The mouse iPS cells growing on hydrophilic surface or collagen showed spreading and flat colonies with an occasional round and raised appearance. These cells showed maximum DNA content of cells cultured on Collagen PS, as determined them by the cell culture assay (Fig. 4).

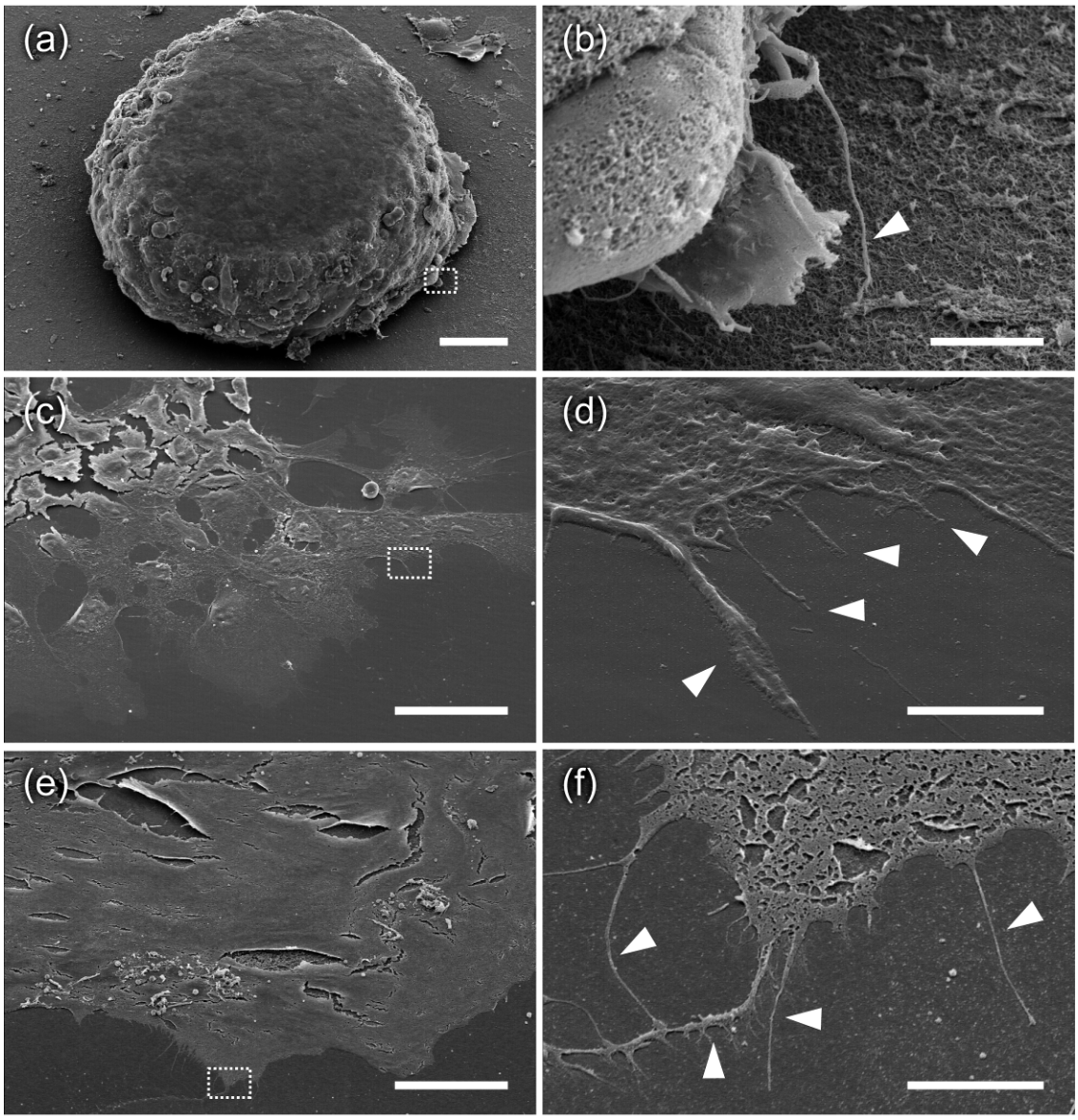

Fig. 6

3.4 *Differentiation state of mouse iPS cells*

Expression of ALP is one of the early undifferentiation markers of iPS cells. To examine the undifferentiated state of the mouse iPS cells, ALP activity in the cells cultured on the dishes was observed by ALP staining. The optical microscope images show the mouse iPS cells stained for ALP activity after 5 d of cultivation on MWCNT5 (Fig. 7a), Culture PS (Fig. 7e), and Collagen PS (Fig. 7i) in the presence of 15% FBS and LIF. Most of the colonies on MWCNT5 stained positive for ALP activity, however, the flat colonies on Culture PS and Collagen PS were partially pale. Further, the undifferentiated state of the mouse iPS cells was determined by the immunological detection of OCT3/4 and Nanog, which are widely used as early undifferentiation markers of mouse iPS cells [2,44]. After 5 d of culture, the mouse iPS cells on MWCNT5, Culture PS, and Collagen PS were stained with DAPI (Fig. 7b, f, and j, respectively; blue), anti-mouse OCT3/4 Alexa Fluor 488 conjugate (Fig. 7c, g, and k, respectively; green), and anti-mouse Nanog Alexa Fluor 647 conjugate (Fig. 7d, h, and l, respectively; red). Most of the cells on MWCNT5 formed dense clusters and stained positive for OCT3/4 and Nanog (Fig. 7, upper row). Although 50% the cells on Culture PS and Collagen PS also formed partially raised colonies and stained positive for OCT3/4 and Nanog, most of the cells spread around the colonies were pale (Fig. 7, middle upper and middle lower row). Although fluorescent spots of OCT3/4, Nanog,

and DAPI were almost co-localized for the cells on MWCNT5 at merge images of immunostaining (Fig. 7m), they were not co-localized for most of the cells on Culture PS and Collagen PS (Fig. 7n and o).

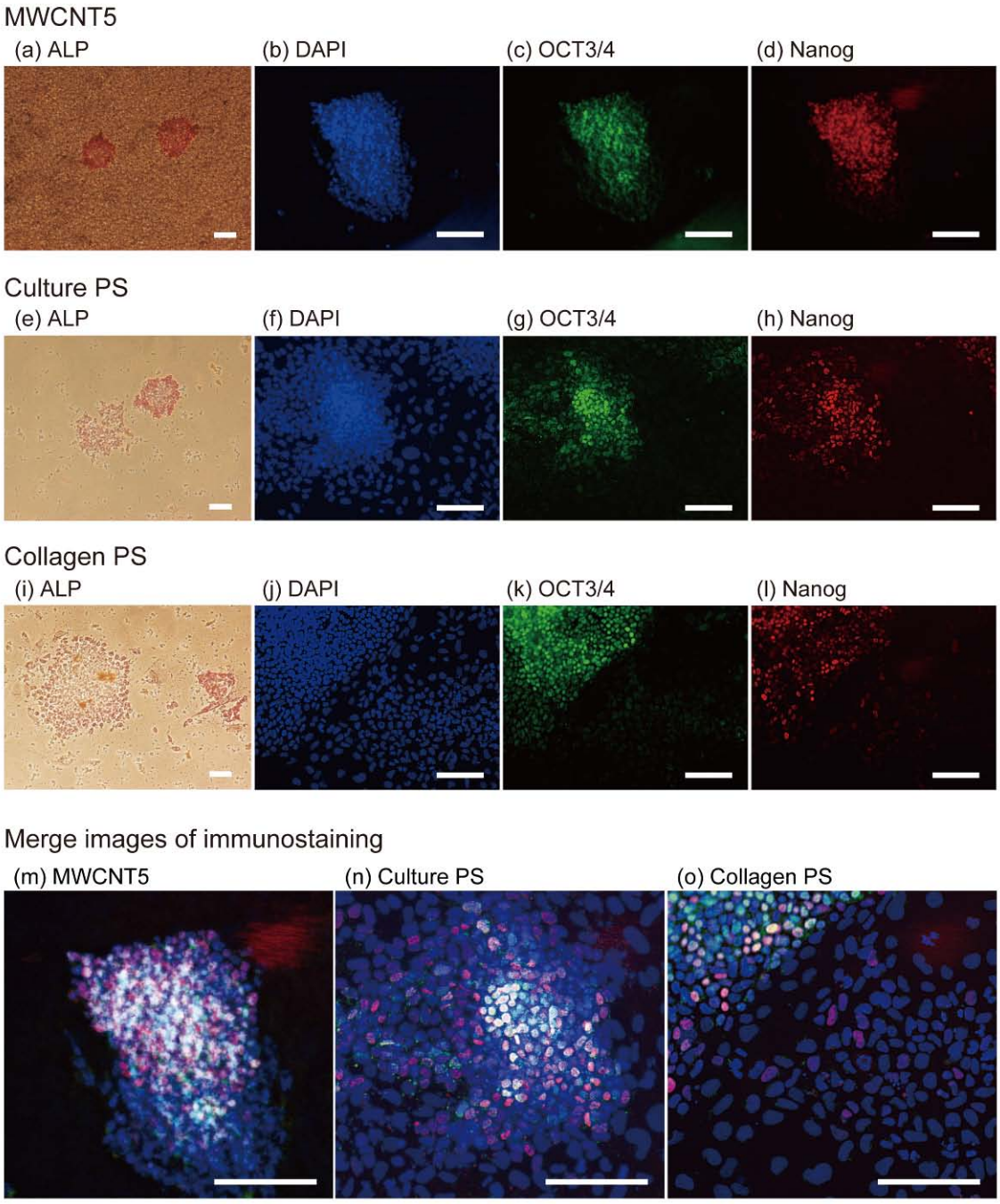

Fig. 7

3.5 *Cell culture assay of MEF-1 cells*

Fig. 8 shows the DNA content of MEF-1 cells cultured on various types of dish substrates for 5 d. The DNA content of the cells cultured on SWCNT0.5 was slightly higher than that on the other CNT-coated dishes. However, the DNA content of the cells cultured on SWCNT0.5, MWCNT0.5, and MWCNT5 was considered similar value; this DNA content was considerably less compared with that on Culture PS and Collagen PS ($p < 0.05$). The DNA content of the cells cultured on Collagen PS was 4.0 times greater than that on MWCNT5 ($p < 0.05$).

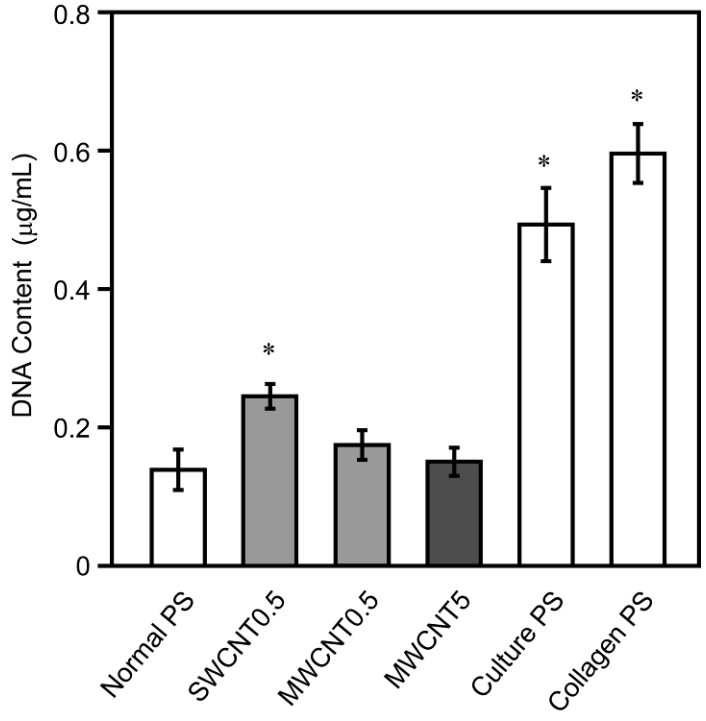

Fig. 8

4. Discussion

Thick MWCNT5 films provided high cell adhesion and hindered spreading of the mouse iPS cells. Cell adhesion (Fig. 2) and morphology (Fig. 3) of the mouse iPS cells on the dish substrates seemed to be strongly influenced by several factors, mainly surface roughness in the case of the CNT-coated dishes and functional groups of the surface in the case of Culture PS and Collagen PS. Cell adhesion increases with increase in the roughness of the surface in a limited range [45–47]. In this study, the surface of thick films of MWCNT5 was rougher with denser 3D network than the surfaces of the thin films of SWCNT0.5 and MWCNT0.5, which were comparatively smooth (Table 1). SWCNT0.5 and MWCNT0.5 showed low adhesiveness; the amount of CNT coating was sufficient for interacting with each iPS cell. Our observations of high adhesion and round shape of the mouse iPS cells on the thick MWCNT films were similar to those of the high adhesion [41] and hindered spreading [23–25] of several types of adherent cells on MWCNT scaffolds. CNTs are composed of graphite and have no functional groups such as -OH and -COOH, except an aromatic group. In this study, MWCNT5, in particular, had a rough surface with a 3D network. This feature of the thick MWCNT5 films apparently provided a genial grip with the 3D network for mouse iPS cell

adhesion. At least, the thick MWCNT5 films showed higher adhesiveness than the thin films because of their rougher surface. Another possibility is that the surface of the MWCNT5 films could show moderate wettability due to their roughness and graphite structure [47]. Further, protein adsorption on CNTs from the serum possibly influences cell adhesion [41] and cell growth [22]. In this case, protein adsorption from the serum supports cell adhesion of the mouse iPS cells on the CNT films to some degree.

The highest adhesion of the mouse iPS cells was observed on Collagen PS (Fig. 2). Collagen or gelatin is a popular matrix for general cell culture and for the culture of ES cells [11,43,48,49] and iPS cells [11,12] under feeder-free conditions. The highest number of adherent mouse iPS cells on Collagen PS recorded in this study was in agreement with that indicating highly efficient adhesion of human ES cells on a collagen-coated surface [48]. However, most of the mouse iPS cells on Collagen PS were spread in all directions after 12 h (Fig. 3c). The observation of cell spreading on Collagen PS at an early stage indicates promotion of cell spreading on the collagen coating after 5 d of incubation, as described below. Collagen molecule may play a role as a ligand for cell adhesion [48] or an adsorbent for cell adhesion proteins [50]. Further, Culture PS showed a similar or slightly less effect on cell adhesion and spreading at the early stage, compared with Collagen PS (Fig. 3b). Normal PS, Culture PS, and Collagen

PS had non-treated, hydrophilic-treated, and collagen-treated surfaces, respectively. The surface of Culture PS had some active groups such as -OH, -C=O, and -COOH and a slight negative charge [51,52]. The surface of Collagen PS had the functional groups of the collagen molecules [53,54]. The functional groups of the dishes largely influenced wettability, and then the surfaces of Culture PS and Collagen PS indicate hydrophilicity (Table 1). Further, it is known that chemical modifications of the surfaces of cell culture substrates largely influence cell adhesion [55–58]. Therefore, the functional groups of the surface of Culture PS would play a role in cell adhesion similar to the functional groups of the collagen molecules. Thus, the results of the cell adhesion assay and the SEM observations indicated surface roughness as a major factor influencing cell adhesion in the case of MWCNT5 and functional groups of the surface as a major factor influencing cell adhesion in the case of Culture PS and Collagen PS.

MWCNT5 showed hemiround colonies of the mouse iPS cells after 5 d of cultivation in 15% FBS and LIF. We observed that the mouse iPS cells tended to grow less on the CNT-coated dishes (Fig. 4) as compared with Culture PS and Collagen PS, and formed hemiround colonies (Fig. 5). Among the CNT-coated dishes, MWCNT5 particularly showed hemiround colonies (Fig. 6a and b) and high cell number. Our previous studies have reported round and elongated shapes of osteoblast-like cells

(Saos-2) cultured on thick CNT films, which were due to the topological effect of the films [22]. Other studies have also shown that cells cultured on MWCNTs tend to acquire a spherical shape [23–25]. The findings agree with our observation of the hemiround shape of the mouse iPS cell colony on MWCNT5 in this study. Tutak et al. reported that the nano-level rough surface of SWCNT films reduces proliferation of osteoblastic cells [47]. Gerecht et al. reported that human ES cells cultured on substrates with nano-topographic features exhibit reduced projected cell area and proliferation [59]. The results of projected cell area and proliferation on substrates with nano-topographic features is similar to those of the formation of hemiround colonies and decreased cell number of the mouse iPS cells on MWCNT5 in this study, compared with the observation on Culture PS and Collagen PS. Therefore, the rough surface of the thick MWCNT films probably inhibited the spreading of the colony of iPS cells in the same way as that for each iPS cell at an early stage, as mentioned above, and decreased cell growth. Comprehensively, from the viewpoint of surface chemistry, these phenomena on CNT-coated dishes would be related with the surface energy or wettability [22,47]. Similar morphology of hemiround colonies was also observed on SWCNT0.5 and MWCNT0.5, however there were considerably few numbers of colonies on them (Fig. 4 and Fig. 5b and c). In the case of SWCNT0.5 and MWCNT0.5, it is difficult to cause

cell adhesion at the first stage of cell growth due to their flatter surfaces than that of MWCNT5 and their mild interaction compared to Culture PS and Collagen PS. Therefore, the cells cultured on SWCNT0.5 and MWCNT0.5 exhibited few numbers of colonies and hemiround at 5 d of cultivation.

Meanwhile, gelatin or occasionally used collagen [1,11] coating is a popular matrix for general cell culture and for the culturing of iPS and ES cells. In this study, we used a collagen-coated PS not a gelatin-coated PS as one of the control substrates for availability and reproducibility of iPS cell culturing [60,61] because collagen molecule is already coated on the surface of a polystyrene dish as a product. Doran et al. reported that a collagen-coated substrate is suitable for human ES cell proliferation [48]. Greenlee et al. reported that mouse ES cells cultured on gelatin spread well and form flat colonies with occasional round and raised appearance [49]. In the present study too, the iPS cells on Collagen PS showed the highest cell number at 5 d (Fig. 4) and good spreading (Fig. 5f and Fig. 6e and f). Moreover, cell spreading on Collagen PS started at an early stage as described above (Fig. 3c). This indicates that the collagen molecules on the dish substrate largely influenced on cell adhesion, spreading, and growth; the flat surface of the substrate did not inhibit cell proliferation. Thus, collagen on the dish induced spreading and growth of the mouse iPS cells in this study. Additionally, Culture

PS showed a similar or slightly less effect on cell spreading and growth as compared with Collagen PS (Fig. 4, Fig. 5e, and Fig. 6c and d). However, this effect of Culture PS and Collagen PS is not suitable for the maintenance of hemiround colonies and undifferentiated state of mouse iPS cells under the applied culture conditions.

Most of the mouse iPS cells cultured on MWCNT5 showed positive expression of early undifferentiation markers (ALP, OCT3/4, and Nanog), characterizing the undifferentiated state of the iPS cells. In addition, the hemiround colonies on MWCNT5 suggest that the cells maintained their undifferentiated state. Most of the colonies on MWCNT5 were positive for ALP activity (Fig. 7a); however, ALP staining of the flat colonies on Culture PS and Collagen PS was partially pale (Fig. 7e and i). Furthermore, OCT3/4 and Nanog expression levels remained higher on MWCNT5 than on Culture PS and Collagen PS (Fig. 7). The expression of all the early undifferentiation markers, namely, ALP, OCT3/4, and Nanog, in the mouse iPS cells on MWCNT5 strongly suggests that MWCNT5 supported the maintenance of a highly undifferentiated iPS cell culture in 15% FBS and LIF until 5 d (Fig. 7, upper row). In the case of Culture PS and Collagen PS, the differentiated cells were large and covered the area between the colonies of the undifferentiated cells (Fig. 7, middle upper and middle lower row). Although fluorescent spots of OCT3/4, Nanog, and DAPI were almost co-localized for

the cells on MWCNT5 at merge images of immunostaining (Fig. 7m), fluorescent spots were not co-localized for most of the cells on Culture PS and Collagen PS (Fig. 7n and o). Localizations of several fluorescent spots of OCT3/4 and Nanog of the cells on all the dishes were slightly difference by detailed observations from merge images. Further study is necessary to investigate slightly difference of expression of OCT3/4 and Nanog of iPS cells. Expression of the early undifferentiation markers in the cells on MWCNT5 seems to be related with the formation of hemiround colonies on MWCNT5, as mentioned above. The results of the strong expression of the early undifferentiation markers in the hemiround mouse iPS cell colonies on MWCNT5 are similar to the previous study results of strong ALP activity in ES cells hemirounded and comparatively weak ALP activity in ES cells spread on gelatin-coated dishes [49]. It is known that chemical modifications of the surfaces of cell culture substrates largely influence cell proliferation and functions [55–58,62]. Moreover, chemical modifications of CNTs strongly enhance adhesion and proliferation of osteoblastic cells [47]. Thus, the maintenance of hemiround colonies and undifferentiated state of the iPS cells on MWCNT5 would be due to the rough surface and graphite structure of the CNTs. MWCNT5 provide a grip for the cells owing to its nano-roughness [22], and the bioinert

substrate gently responded to the iPS cells owing to the culturing due to graphite structure [33,34].

Cell number of MEF-1 cells cultured on the CNT-coated dishes was considerably lower than that on Culture PS and Collagen PS at 5 d of cultivation. In general, feeder cells such as MEF or SNL cells are often used in the initial derivation and maintenance of iPS cells [1,3,6]. However, iPS cells containing feeder cells are often problematic for experimental manipulation and subsequent biological assay of the cells [11]. To estimate the cell growth of MEF-1 cells on the CNT-coated dishes, we carried out a cell culture assay. Cell number of MEF-1 cells cultured on the CNT-coated dishes and Normal PS was lesser than that on Culture PS and Collagen PS (Fig. 8). Price et al. reported that proliferation of fibroblasts is decreased by the rough surfaces of carbon materials [63]. MEF-1 cells did not responsed well to both the hydrophobic property and the rough surfaces of the CNT-coated dishes. Ratio of cell number of MEF-1 cells on MWCNT5 (compared with Collagen PS) was considerably lower than that of the mouse iPS cells on MWCNT5 (compared with Collagen PS) (Fig. 4). MEF cells are known to grow well on collagen- or gelatin-coated dishes [64,65]. These results indicate that MWCNT5 decreased the growth of MEF-1 feeder cells and retained the hemiround mouse iPS cells colonies at 5 d of cultivation. Meanwhile, Collagen PS

induced the growth of both the mouse iPS cells and MEF-1 cells. Thus, our results indicate that MWCNT5 can be an effective material for the culturing of mouse iPS cells, retaining the shape of their hemiround colonies, and decreasing the growth of MEF-1 cells. An additional advantage of the culturing of mouse iPS cells on MWCNT5 is that culturing can be done for future experimental manipulations such as gene transfection and toxicity assays without the influence of feeder cells.

In summary, our results indicated that the mouse iPS cells cultured on MWCNT5 formed hemiround colonies and maintained their undifferentiated state in a medium containing 15% FBS and LIF. MWCNT5 provided a grip for the cells owing to its nano-roughness, and the bioinert substrate gently responded to the cells owing to its graphite structure. In addition, growth of MEF-1 cells on MWCNT5 was considerably low as compared with that on Culture PS and Collagen PS. Although further research will be required to characterize the pluripotency of mouse iPS cells cultured on CNT-coated dishes, we conclude that MWCNT5 can be an effective substrate for the maintenance of mouse iPS cells cultured under feeder-free conditions.

5. Conclusion

We demonstrated that the thick MWCNT5 films could maintain hemiround colonies and undifferentiated state of the mouse iPS cells in vitro. The behavior of the mouse iPS cells on the CNT-coated dishes was evaluated by cell adhesion and proliferation (cell culture) assays. The differentiation level of the cells was determined on the basis of the morphological changes and expression of early undifferentiation markers, namely, ALP, OCT3/4, and Nanog. In the cell adhesion assay, the thick MWCNT5 films showed high adhesiveness similar to Culture PS, and slightly lower than Collagen PS. The mouse iPS cells cultured on the thick MWCNT5 films formed hemiround colonies and maintained their undifferentiated state despite decrease cell number as compared with Culture PS and Collagen PS after 5 d. However, the mouse iPS cells cultured on Culture PS and Collagen PS showed a tendency to spread and weakly expressed the early undifferentiation markers. In addition, cell number of MEF-1 cells cultured on MWCNT5 was considerably low as compared with that on Collagen PS at 5 d of cultivation. Our study suggests that thick MWCNT5 films can be used as a substrate for the maintenance of hemiround colonies and undifferentiated state of mouse iPS cells cultured in a medium containing 15% FBS and LIF under feeder-free conditions.

Acknowledgements

We would like to thank OPEN FACILITY (Hokkaido University Sousei Hall) for allowing us to use AFM measurement on the surface of the dishes, especially Dr. Jin Shigeki for his great technical assistant and helpful suggestions. This work was partly funded by “Collaborative Development of Innovative Seeds, Potentiality Verification Stage” from the Japan Science and Technology Agency (JST) and by a Grant-in-Aid for Scientific Research (No. 22791919) from the Ministry of Education, Culture, Sports, Science and Technology of Japan.

References

[1] Takahashi K, Okita K, Nakagawa M, Yamanaka S. Induction of pluripotent stem cells from fibroblast cultures. Nat Protoc 2007;2(12):3081-9.

[2] Okita K, Ichisaka T, Yamanaka S. Generation of germline-competent induced pluripotent stem cells. Nature 2007;448(7151):313-8.

[3] Yu J, Vodyanik MA, Smuga-Otto K, Antosiewicz-Bourget J, Frane JL, Tian S, et al. Induced pluripotent stem cell lines derived from human somatic cells. Science 2007;318(5858):1917-20.

[4] Vojnits K, Bremer S. Challenges of using pluripotent stem cells for safety assessments of substances. Toxicology 2010;270(1):10-7.

[5] Yamashita JK. ES and iPS cell research for cardiovascular regeneration. Exp Cell Res 2010;316(16):2555-9.

[6] Pan C, Hicks A, Guan X, Chen H, Bishop CE. SNL fibroblast feeder layers support derivation and maintenance of human induced pluripotent stem cells. J Genet Genomics 2010;37(4):241-8.

[7] Abraham S, Sheridan SD, Laurent LC, Albert K, Stubban C, Ulitsky I, et al. Propagation of human embryonic and induced pluripotent stem cells in an indirect co-culture system. Biochem Biophys Res Commun 2010;393(2):211-6.

[8] Wu Y, Zhang Y, Mishra A, Tardif SD, Hornsby PJ. Generation of induced pluripotent stem cells from newborn marmoset skin fibroblasts. Stem Cell Res 2010;4(3):180-8.

[9] Masaki H, Ishikawa T, Takahashi S, Okumura M, Sakai N, Haga M, et al. Heterogeneity of pluripotent marker gene expression in colonies generated in human iPS cell induction culture. Stem Cell Res 2008;1(2):105-15.

[10] Hwang ST, Kang SW, Lee SJ, Lee TH, Suh W, Shim SH, et al. The expansion of human ES and iPS cells on porous membranes and proliferating human adipose-derived feeder cells. Biomaterials 2010;31(31):8012-21.

[11] Kitajima H, Niwa H. Clonal expansion of human pluripotent stem cells on gelatin-coated surface. Biochem Biophys Res Commun 2010;396(4):933-8.

[12] Ueda T, Yamada T, Hokuto D, Koyama F, Kasuda S, Kanehiro H, et al. Generation of functional gut-like organ from mouse induced pluripotent stem cells. Biochem Biophys Res Commun 2010;391(1):38-42.

[13] Hirami Y, Osakada F, Takahashi K, Okita K, Yamanaka S, Ikeda H, et al. Generation of retinal cells from mouse and human induced pluripotent stem cells. Neurosci Lett 2009;458(3):126-31.

[14] Akasaka T, Watari F, Sato Y, Tohji K. Apatite formation on carbon nanotubes. Mater Sci Eng C 2006;26(4):675-8.

[15] Mattson MP, Haddon RC, Rao AM. Molecular functionalization of carbon nanotubes and use as substrates for neuronal growth. J Mol Neurosci 2000;14(3):175-82.

[16] Tran PA, Zhang L, Webster TJ. Carbon nanofibers and carbon nanotubes in regenerative medicine. Adv Drug Deliv Rev 2009;61(12):1097–114.

[17] Harrison BS, Atala A. Carbon nanotube applications for tissue engineering. Biomaterials 2007;28(2):344-53.

[18] Cheung W, Pontoriero F, Taratula O, Chen AM, He H. DNA and carbon nanotubes as medicine. Adv Drug Deliv Rev 2010;62(6):633-49.

[19] Zhang Y, Bai Y, Yan B. Functionalized carbon nanotubes for potential medicinal applications. Drug Discov Today 2010;15(11-12):428-35.

[20] Akasaka T, Watari F. Capture of bacteria by flexible carbon nanotubes. Acta Biomater 2009;5(2):607-12.

[21] Tay CY, Gu H, Leong WS, Yu H, Li HQ, Heng BC, et al. Cellular behavior of human mesenchymal stem cells cultured on single-walled carbon nanotube film. Carbon 2010;48(4):1095-1104.

[22] Akasaka T, Yokoyama A, Matsuoka M, Hashimoto T, Watari F. Thin films of single-walled carbon nanotubes promote human osteoblastic cells (Saos-2) proliferation in low serum concentrations. Mater Sci Eng C 2010;30(3):391-9.

[23] Mwenifumbo S, Shaffer MS, Stevens MM. Exploring cellular behaviour with multi-walled carbon nanotube constructs. J Mater Chem 2007;17(19):1894-902.

[24] Zhang X, Wang X, Lu Q, Fu C. Influence of carbon nanotube scaffolds on human cervical carcinoma HeLa cell viability and focal adhesion kinase expression. Carbon 2008;46(3):453-60.

[25] George JH, Shaffer MS, Stevens MM. Investigating the cellular response to nanofibrous materials by use of a multi-walled carbon nanotube model. J Exp Nanosci 2006;1(1):1-12.

[26] Matsuoka M, Akasaka T, Totsuka Y, Watari F. Strong adhesion of Saos-2 cells to multi-walled carbon nanotubes. Mater Sci Eng B 2010;173(1-3):182-6.

[27] Aoki N, Yokoyama A, Nodasaka Y, Akasaka T, Uo M, Sato Y, et al. Strikingly extended morphology of cells grown on carbon nanotubes. Chem Lett 2006;35(5):508-9.

[28] Lobo AO, Antunes EF, Machado AHA, Pacheco-Soares C, Trava-Airoldi VJ, Corat EJ. Cell viability and adhesion on as grown multi-wall carbon nanotube films. Mater Sci Eng C 2008;28(2):264-9.

[29] Kalbacova M, Kalbac M, Dunsch L, Hempel U. Influence of single-walled carbon nanotube films on metabolic activity and adherence of human osteoblasts. Carbon 2007;45(11):2266-72.

[30] Gott VL, Whiffen JD, Dutton RC. Heparin bonding on colloidal graphite surfaces. Science 1963;142:1297-8.

[31] Fitzer E. The future of carbon-carbon composites. Carbon 1987;25(2):163-90.

[32] Fiorito S, Serafino A, Andreola F, Bernier P. Effects of fullerenes and single-wall carbon nanotubes on murine and human macrophages. Carbon 2006;44(6):1100-5.

[33] Jenkins GM, de Carvalho FX. Biomedical applications of carbon fibre reinforced carbon in implanted prostheses. Carbon 1977;15(1):33-7.

[34] Bokros JC. Carbon biomedical devices. Carbon 1977;15(6):355-71.

[35] Zhu L, Chang DW, Dai L, Hong Y. DNA damage induced by multiwalled carbon nanotubes in mouse embryonic stem cells. Nano Lett 2007;7(12):3592-7.

[36] Sridharan I, Kim T, Wang R. Adapting collagen/CNT matrix in directing hESC differentiation. Biochem Biophys Res Commun 2009;381(4):508-12.

[37] Chao TI, Xiang S, Chen CS, Chin WC, Nelson AJ, Wang C, et al. Carbon nanotubes promote neuron differentiation from human embryonic stem cells. Biochem Biophys Res Commun 2009;384(4):426-30.

[38] Zhao X, Inoue S, Jinno M, Suzuki T, Ando Y. Macroscopic oriented web of single-wall carbon nanotubes. Chem Phys Lett 2003;373(3-4):266-71.

[39] Sato Y, Yokoyama A, Shibata K, Akimoto Y, Ogino S, Nodasaka Y, et al. Influence of length on cytotoxicity of multi-walled carbon nanotubes against human acute monocytic leukemia cell line THP-1 *in vitro* and subcutaneous tissue of rats *in vivo*. Mol Biosyst 2005;1(2):176-82.

[40] Stalder AF, Kulik G, Sage D, Barbieri L, Hoffmann P. A snake-based approach to accurate determination of both contact points and contact angles. Colloids and Surfaces A: Physicochem Eng Aspects 2006;286(1-3):92-103.

[41] Akasaka T, Yokoyama A, Matsuoka M, Hashimoto T, Abe S, Uo M, et al. Adhesion of human osteoblast-like cells (Saos-2) to carbon nanotube sheets. Biomed Mater Eng 2009;19(2-3):147-53.

[42] Datta N, Holtorf HL, Sikavitsas VI, Jansen JA, Mikos AG. Effect of bone extracellular matrix synthesized in vitro on the osteoblastic differentiation of marrow stromal cells. Biomaterials 2005;26(9):971-7.

[43] Rose TM, Weiford DM, Gunderson NL, Bruce AG. Oncostatin M (OSM) inhibits the differentiation of pluripotent embryonic stem cells in vitro. Cytokine 1994;6(1):48-54.

[44] Tokumoto Y, Ogawa S, Nagamune T, Miyake J. Comparison of efficiency of terminal differentiation of oligodendrocytes from induced pluripotent stem cells versus embryonic stem cells in vitro. J Biosci Bioeng 2010;109(6):622-8.

[45] Le Guehennec L, Lopez-Heredia MA, Enkel B, Weiss P, Amouriq Y, Layrolle P. Osteoblastic cell behaviour on different titanium implant surfaces. Acta Biomater 2008;4(3):535-43.

[46] Bigerelle M, Anselme K, Noël B, Ruderman I, Hardouin P, Iost A. Improvement in the morphology of Ti-based surfaces: a new process to increase in vitro human osteoblast response. Biomaterials 2002;23(7):1563-77.

[47] Tutak W, Chhowalla M, Sesti F. The chemical and physical characteristics of single-walled carbon nanotube film impact on osteoblastic cell response. Nanotechnology 2010;21(31):315102.

[48] Doran MR, Frith JE, Prowse ABJ, Fitzpatrick J, Wolvetang EJ, Munro TP, et al. Defined high protein content surfaces for stem cell culture. Biomaterials 2010;31(19):5137-42.

[49] Greenlee AR, Kronenwetter-Koepel TA, Kaiser SJ, Liu K. Comparison of Matrigel™ and gelatin substrata for feeder-free culture of undifferentiated mouse embryonic stem cells for toxicity testing. Toxicol In Vitro 2005;19(3):389-97.

[50] Kleinman HK, Klebe RJ, Martin GR. Role of collagenous matrices in the adhesion and growth of cells. J Cell Biol 1981;88(3):473-85.

[51] Curtis ASG, Forrester JV, McInnes C, Lawrie F. Adhesion of cells to polystyrene surfaces. J Cell Biol 1983;97(5):1500-6.

[52] Onyiriuka EC, Hersh LS, Hertl W. Solubilization of corona discharge- and plasma-treated polystyrene. J Colloid Interface Sci 1991;144(1):98-102.

[53] Kurotobi K, Kaibara M, Suzuki Y, Iwaki M, Nakajima H, Kaneko S. Ion implantation into collagen-coated surfaces for the development of small diameter artificial grafts. Colloids Surf B Biointerfaces 2000;19(3):227-35.

[54] Veis A. Collagen fibrillogenesis. Connect Tissue Res 1982;10(1):11-24.

[55] Kim MH, Kino-oka M, Taya M. Designing culture surfaces based on cell anchoring mechanisms to regulate cell morphologies and functions. Biotechnol Adv 2010;28(1):7-16.

[56] Faucheux N, Schweiss R, Lützow K, Werner C, Groth T. Self-assembled monolayers with different terminating groups as model substrates for cell adhesion studies. Biomaterials 2004;25(14):2721-30.

[57] Schamberger PC, Gardella JA. Surface chemical modifications of materials which influence animal cell adhesion—a review. Colloids Surf B Biointerfaces 1994;2(1-3):209-23.

[58] Ma Z, Mao Z, Gao C. Surface modification and property analysis of biomedical polymers used for tissue engineering. Colloids Surf B Biointerfaces 2007;60(2):137-57.

[59] Gerecht S, Bettinger CJ, Zhang Z, Borenstein JT, Vunjak-Novakovic G, Langer R. The effect of actin disrupting agents on contact guidance of human embryonic stem cells. Biomaterials 2007;28(2):4068-77.

[60] Narazaki G, Uosaki H, Teranishi M, Okita K, Kim B, Matsuoka S, et al. Directed and systematic differentiation of cardiovascular cells from mouse induced pluripotent stem cells. Circulation 2008;118(5):498-506.

[61] Stadtfeld M, Apostolou E, Akutsu H, Fukuda A, Follett P, Natesan S, et al. Aberrant silencing of imprinted genes on chromosome 12qF1 in mouse induced pluripotent stem cells. Nature 2010;465(7295):175-181.

[62] Phillips JE, Petrie TA, Creighton FP, García AJ. Human mesenchymal stem cell differentiation on self-assembled monolayers presenting different surface chemistries. Acta Biomater 2010;6(1):12-20.

[63] Price RL, Ellison K, Haberstroh KM, Webster TJ. Nanometer surface roughness increases select osteoblast adhesion on carbon nanofiber compacts. J Biomed Mater Res A 2004;70(1):129-38.

[64] Nur-E-Kamal A, Ahmed I, Kamal J, Schindler M, Meiners S. Three-dimensional nanofibrillar surfaces promote self-renewal in mouse embryonic stem cells. Stem Cells 2006;24(2):426-33.

[65] Okada M, Oka M, Yoneda Y. Effective culture conditions for the induction of pluripotent stem cells. Biochim Biophys Acta 2010;1800(9):956-63.

Figure captions:

Fig. 1. SEM images of the surface of various types of the dish substrates. (a) non-treated polystyrene (Normal PS), (b) thin film (0.5 μg/cm^2) of SWCNTs (SWCNT0.5), (c) thin film (0.5 μg/cm^2) of MWCNTs (MWCNT0.5), (d) thick films (0.5 μg/cm^2) of MWCNTs (MWCNT5), (e) cell culture polystyrene (Culture PS), and (f) collagen-coated polystyrene (Collagen PS). Scale bar: 1 μm.

Fig. 2. DNA content of cells adhering on the surfaces of various types of dish substrates, calculated via a cell adhesion assay. Mouse iPS cells were incubated on Normal PS, SWCNT0.5 (0.5 μg/cm^2), MWCNT0.5 (0.5 μg/cm^2), MWCNT5 (5 μg/cm^2), Culture PS, and Collagen PS in DMEM containing 15% FBS and LIF for 1 h. Error bars indicate a standard error for $n = 4$. Asterisks indicate statistical significance ($p < 0.05$), compared with MWCNT5.

Fig. 3. SEM images of mouse iPS cells adhering to the surfaces of (a) MWCNT5 (5 μg/cm^2), (b) Culture PS, and (c) Collagen PS. Mouse iPS cells were incubated in DMEM containing 15% FBS and LIF for 12 h. Scale bar: 20 μm.

Fig. 4. Mouse iPS cell growth on various types of dish substrates. Mouse iPS cells were cultured on Normal PS, SWCNT0.5 (0.5 μg/cm^2), MWCNT0.5 (0.5 μg/cm^2), MWCNT5 (5 μg/cm^2), Culture PS, and Collagen PS in DMEM containing 15% FBS and LIF for 5 d. DNA content of 4-mL lysate in each dish was estimated by the PicoGreen DNA assay. Cell growth was assayed by DNA content on the dishes. Error bars indicate a standard error for $n = 4$. Asterisks indicate statistical significance ($p < 0.05$), compared with MWCNT5.

Fig. 5. Optical microscope images of mouse iPS cells on various types of dish substrates after incubation for 5 d. Mouse iPS cells were cultured on (a) Normal PS, (b) SWCNT0.5 (0.5 μg/cm^2), (c) MWCNT0.5 (0.5 μg/cm^2), (d) MWCNT5 (5 μg/cm^2), (e) Culture PS, and (f) Collagen PS. Scale bar: 100 μm.

Fig. 6. SEM images of mouse iPS cells on MWCNT5, Culture PS, and Collagen PS after culturing for 5 d. (a) MWCNT5 (5 μg/cm^2), (b) MWCNT5 (5 μg/cm^2) at higher magnification, (c) Culture PS, and (d) Culture PS at higher magnification, (e) Collagen PS, and (f) Collagen PS at higher magnification. The area enclosed in the small white

squares of dotted lines was observed at higher magnification. White triangles indicate the filopodia of the cells. Scale bar: left side, 50 μm; right side, 5 μm.

Fig. 7. ALP staining and immunostaining of mouse iPS cells cultured on MWCNT5 (5 μg/cm^2) (upper row), Culture PS (middle upper row), and Collagen PS (middle lower row). Mouse iPS cells were cultured in DMEM containing 15% FBS and LIF for 5 d. The cells were stained with ALP staining solution (a, e, and i). Scale bar: 200 μm. The panels b, f, and j show nuclear staining by DAPI (blue). The panels c, g, and k show staining with anti-mouse OCT3/4 Alexa Fluor 488 (green). The panels d, h, and l show staining with anti-mouse Nanog Alexa Fluor 647 (red). The panels m, n, and o show merge images of immunostaining on MWCNT5, Culture PS, and Collagen PS, respectively. Scale bar: 100 μm.

Fig. 8. DNA content of MEF-1 cell cultured on various types of dish substrates. MEF-1 cells were cultured on Normal PS, SWCNT0.5 (0.5 μg/cm^2), MWCNT0.5 (0.5 μg/cm^2), MWCNT5 (5 μg/cm^2), Culture PS, and Collagen PS in DMEM containing 10% FBS for 5 d. Error bars indicate a standard error for n = 4. Asterisks indicate statistical significance ($p < 0.05$), compared with MWCNT5.